Solution-processable ambipolar organic field-effect transistor based on Co-planar bisphthalocyaninato copper

Yan Shi, Xiyou Li *

Key Laboratory of Colloid and Interface Chemistry, Ministry of Education, Department of Chemistry, Shandong University, Jinan 250100, China

ABSTRACT

A soluble binuclear phthalocyaninato copper (II) complex, $Cu_2[Pc(COOC_8H_{17})_6]_2$ (**1**), with planar molecular structure and extended conjugation system, has been designed and synthesized. By fusing two phthalocyanine rings side by side and introducing electron withdrawing groups at periphery positions, the energy levels of HOMO and LUMO have been tuned successfully into the range of an air-stable ambipolar organic semiconductor required as revealed by the electrochemical studies. With the help of a solution-based quasi-Langmuir–Shäfer (QLS) method, thin solid films of this compound were fabricated and organic field effect transistors (OFETs) based on these QLS thin solid films were constructed. Because of the promising electrochemical properties as well as the high ordered packing structure of the molecules in the thin solid films, the OFETs performed excellent ambipolar operating properties, with the electron and hole mobility in air as high as 1.7×10^{-1} and $2.3 \times 10^{-4} \, cm^2 \, V^{-1} \, s^{-1}$, respectively. For comparison purpose, mononuclear compound $Cu[Pc(COOC_8H_{17})_8]$ (**2**) was comparatively studied. The QLS thin solid films of this compound possess similar ordered structure with that of $Cu_2[Pc(COOC_8H_{17})_6]_2$ (**1**), but the OFETs based on the thin solid films of this compound can only show n-type properties under nitrogen atmosphere with an extremely small electron mobility of $1.6 \times 10^{-4} \, cm^2 \, V^{-1} \, s^{-1}$. This result suggests that extension on the conjugation system of an aromatic compound with multiple electron withdrawing groups can tune the molecule into an air stable ambipolar organic semiconductor.

© 2013 Elsevier B.V. All rights reserved.

1. Introduction

The development of solution-processable organic semiconductors for the thin-film organic field effect transistors (OFETs), which exhibit high carrier mobility and good ambient stability, is crucial to realizing low-cost and mechanically flexible printed electronics [1–4]. During the past decade, intensive researches towards developing novel semiconductor materials especially those possessing π-conjugated electronic structure including conjugated polymers, oligomeric thiophenes, linear fused acenes, perylenes, and phthalocyanines have yielded a number of transistors with either hole or electron as the charge car-rier [5–14]. But ambipolar OTFTs, which allow dual operation at both p and n channel, are highly desired for practical applications in integrated circuits like high gain complementary metal-oxide–semiconductor inverters and light emitting devices [15–18].

Phthalocyanines (Pcs) with planar or nearly planar molecular structures and a large network of π-electrons have been among the most promising semiconducting materials for OFETs due to their excellent thermal and chemical stabilities and good semiconducting properties. Pcs employed as semiconductors in OFETs can be divided into two categories based on their molecular structures. The first group of phthalocyanines are the commercially available unsubstituted monomeric phthalocyaninato metal complexes (MPc, M = Cu, Co, Fe, Mn, Ni, Zn, etc.) [5]. Among which, CuPc is the most widely used material for

* Corresponding author. Tel.: +86 531 88369877.
E-mail address: xiyouli@sdu.edu.cn (X. Li).

OFETs with hole transfer mobilities in the range of 10^{-5}–1.0 cm^2 V^{-1} s^{-1} [19,20]. The second group of Pcs used in OFETs are the substituted phthalocyanines with reasonable solubilities in conventional organic solvents and can be processed with solution methods, such as amino-(tri-*tert*-butyl)phthalocyaninato copper [21], hydroxyde-cyloxy-(tri-*tert*-butyl) phthalocyaninato copper [22], and sandwich-type bis/tris(phthalocyaninato) rare earth double/triple-decker complexes bearing substituents at the peripheral positions [23]. Most of the Pcs used in OFETs present p-type semiconducting properties with hole as the major charge carriers. Because n-type of OFETs are important for the implementation of complementary circuits, which have low power consumption, high operating speeds, and an increased device lifetime, but n-type organic semiconductors have significantly lagged behind their p-type counterparts [10,11,24]. As a result, design and synthesis of n-type or ambipolar phthalocyanine based semiconductors with acceptable performance and robust air stability has become an fasinating area in the past decade. Pioneer work of Bao and co-workers in this field demonstrated that the CuPc can be changed successfully into air stable n-type semiconductor by introducing sixteen fluorine atoms on the periphery positions of the phthalocyanine ring (copper hexadecafluorophthalocyanine, F$_{16}$CuPc) with mobility as high as 0.03 cm^2 V^{-1} s^{-1} [25]. Since than F$_{16}$CuPc becomes a widely applied n-type semiconductor in different OFETs with different structures [26–28]. However, because F$_{16}$CuPc cannot dissolve in conventional organic solvents, and therefore, the OFETs based on this material are all fabricated by vacuum deposition techniques. Very recently, solution processable monomeric phthalocyaninato copper and "sandwich" type phthalocyaninato rare earth metal complexes have been successfully changed into n-type or ambipolar semiconductors by attaching electron withdrawing groups [29]. The ambipolar semiconductors are particularly important because they can fabricated into ambipolar OFETs based on only one semiconducting component, which ensures a simple device structure and low-cost fabrication, have therefore attracted great research interest [30,31]. However, the ambipolar semiconductors with reasonable semiconducting properties are still rare, the design and synthesis of novel ambipolar solution processable phthalocyanine semiconductor remain a challenge for phthalocyanine chemists and material scientists.

For organic semiconductors with conjugated electronic structure, the energy of the lowest unoccupied molecular orbitals (LUMOs), that are necessary for ensuring effective electron injection and stable electron transport under ambient conditions, should locate below −4.0 eV, while that of the highest occupied molecular orbitals (HOMOs) should align with the work function of air-stable electrodes (Au: 5.1 eV) for the purpose of diminishing the hole injection barrier [32–34]. Hence, the key problem in searching for good ambipolar organic semiconductors should be tuning the energy levels of HOMO and LUMO, and meanwhile reaching a delicate balance between solubility in conventional organic solvents and efficient molecular packing behavior in solid state. In the present paper, we designed a novel bisphthalocyaninato copper complex,

Cu$_2$[Pc(COOC$_8$H$_{17}$)$_6$]$_2$ (**1**), Scheme 1. Carboxylate groups are introduced to the bisphthalocyanine periphery positions, which on one the hand can improve the solubilities of this bisphhtalocyanine compound in conventional organic solvents, on the other hand they are electron withdrawing groups and can lower the energy levels of LUMO and are expected to tune the semiconducting nature of phthalocyaninato copper complexes from p-type to n-type [29]. Most importantly, the extra large π-conjugation net work is expected to increase the energy of HOMO significantly [35], and then makes it matches with the work function of Au electrode. Moreover, the extended π system could enhance the π–π interactions between neighbor molecules in solid state and thus could improve the carrier mobility. To the best of our knowledge, this represents the first experimental effort towards developing organic semiconductors based on bisphthalocyaninato metal complexes. More importantly, this work proves that extending on the conjugation system of molecule will be powerful approach to tune the semiconducting properties of phthalocyanines.

2. Experimental section

2.1. General methods

Electronic absorption spectra and polarized UV–vis absorption spectra were recorded on a SHIMADZU UV-2450. X-ray diffraction experiments were carried out on a Rigaku D/max-gB X-ray diffractometer. MALDI-TOF mass spectra were taken on a Bruker BIFLEX III instrument. Substrates for the thin solid film deposition were successively cleaned with pure water, acetone, and ethanol. Electrochemical measurements were carried out with a chenhua-760 voltammetric analyzer. The cell comprised inlets for a glassy carbon disk working electrode of 2.0 mm in diameter and a silver wire counter electrode. The reference electrode was Ag/Ag$^+$ (a solution of 0.01 M AgNO$_3$ and 0.1 M TBAP in acetonitrile), which was connected to the solution by a Luggin capillary whose tip was placed close to the working electrode. It was corrected for junction potentials by being referenced internally to the ferrocenium/ferrocene Fc$^+$/Fc) couple. Typically, a 0.1 M solution of [NBu$_4$][ClO$_4$] in CH$_2$Cl$_2$ containing 0.5 M of sample was purged with nitrogen for 10 min, and then the voltammograms were recorded at ambient temperature. The scan rates were 20 and 10 mV s^{-1} for cyclic voltammetry (CV) and differential pulse voltammetry (DPV), respectively.

2.2. OFET device fabrication

The thin solid films were deposited by the solution-based quasi-Langmuir–Shäfer (QLS) method [36]. Before the film deposition, surface treatment with HMDS for SiO$_2$/Si substrates was performed according to literature method [37]. OTFT devices were fabricated on a HMDS treated Si/SiO$_2$ (300 nm thickness, capacitance C$_0$ = 10 nF cm^{-2}) substrate by evaporating gold electrodes onto the QLS films of Cu$_2$BPc employing a shadow mask.
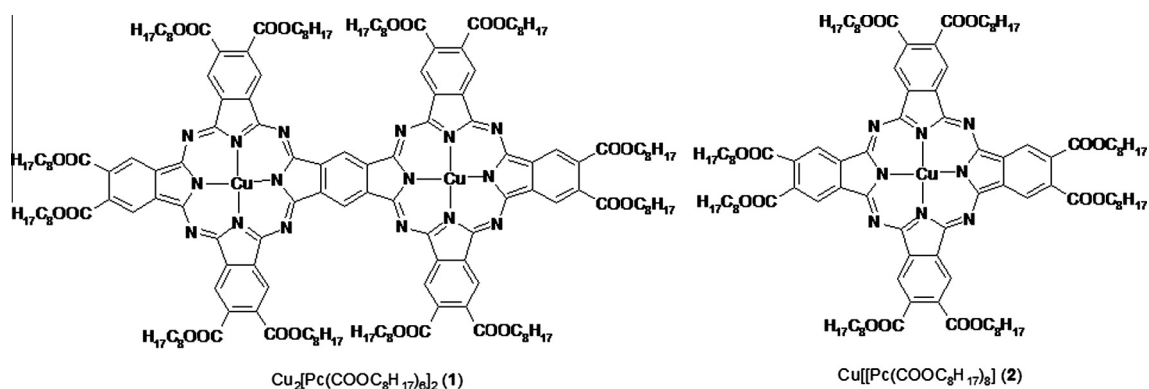
Scheme 1. Molecular structure of Cu$_2$[Pc(COOC$_8$H$_{17}$)$_6$]$_2$ (**1**) and Cu[Pc(COOC$_8$H$_{17}$)$_8$] (**2**).

Electrodes with two sets of dimensions (W = 8.16 mm, L = 145 μm, W/L = 56 and W = 28.6 mm, L = 240 lm, W/L = 119) were used for OFET measurements. The drain–source current (I_{ds}) versus drain–source voltage (V_{ds}) characteristic was obtained with a Hewlett-Packard (HP) 4140B parameter analyzer at room temperature.

2.3. Materials and synthesis

Reference compound copper-phthalocyanine Cu[Pc(COOC$_8$H$_{17}$)$_8$] (**2**) was synthesized by the method of literature [38]. Hexamethyldisilazane (HMDS) was purchased from Aldrich. All other reagents and solvents were of reagent grade and used as received.

Cu$_2$[Pc(COOC$_8$H$_{17}$)$_6$]$_2$ (**1**) Copper sulphate pentahydrate (2.03 g, 12.72 mmol), pyromellitic dianhydride (3.2 g, 14.67 mmol), urea (10 g, 167 mmol), ammonium chloride (0.83 g, 15.51 mmol), and ammonium molybdate (0.24 g, 0.19 mmol) were ground together and then placed in a three flask containing nitrobenzene. The flask was heated to 185 °C and maintained at this temperature for 12 h. The obtained solid material was boiled with hydrochloric acid, and then treated with potassium hydroxide. The final powder was dried at room temperature under vacuum. The dried product was dissolved in n-octyl alcohol with p-toluenesulfonic acid (100 mg, 0.53 mmol) as catalyst. The temperature of the three necked flask was gradually increased to 180–185 °C and maintained at this temperature for 12 h. After remove the solvents under reduced pressure, the obtained solid was finely ground and washed with methanol until it was free of n-octyl alcohol. The residue was purified by column chromatography on silica gel using CHCl$_3$/methanol (99.5:0.5) as eluent. The first green band contains the reference **2**. (33 mg, 33%) Compound **1** was recovered from the second blue band (7 mg, 2.3%). Repeated chromatography followed by recrystallization from CHCl$_3$ and MeOH gave pure **1** as blue powder. MS (MALDI-TOF) calculated for: C$_{184}$H$_{258}$Cu$_2$N$_8$O$_{24}$, 3091.1, Found 3091.8 [M$^+$]; Elemental analysis: calculated for C$_{184}$H$_{258}$Cu$_2$N$_8$O$_{24}$; C 71.45%, H 8.41%, N 3.62%, found, C 71.4%, H 8.52%. N 3.65%; UV–vis (CHCl$_3$): λ_{max}/nm (logε), 355 (4.18), 690 (2.61), 734 (3.20), 759 (5.07), 824 (5.24).

3. Results and discussion

3.1. UV–vis absorption and polarized UV–vis spectra

The electronic absorption spectra of **1** and **2** in CHCl$_3$ and the QLS films were recorded and shown in Fig. 1. **2** presents typical electronic absorption spectrum for monomeric phthalocyaninato metal complexes in solution [29a], with the maximal absorption band around 700 nm and a small broad band around 350 nm. But in the spectrum of **1** in solution, a group of absorption bands are observed at 690, 734, 759 and 824 nm, which can be
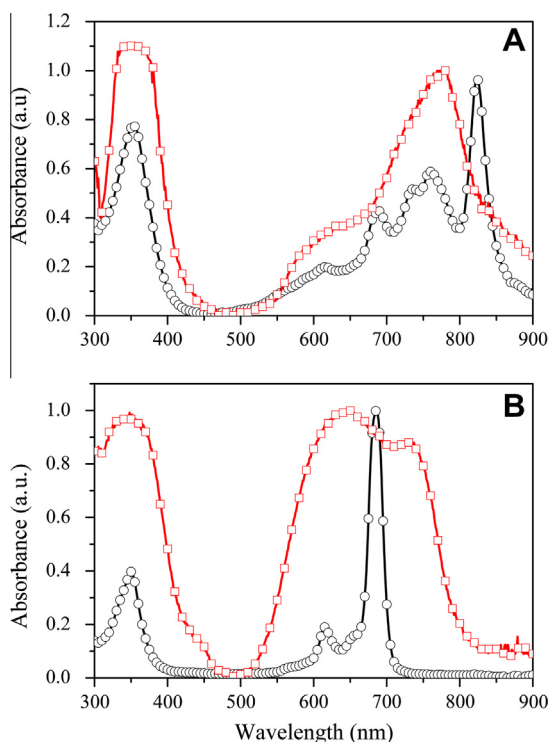

Fig. 1. Normalized electronic absorption spectra of **1** (A) and **2** (B) in CHCl$_3$ (open circle) and QLS films (open square).

assigned to the split Q bands caused by the *D2h* symmetry of the molecule of **1** [39]. Comparing with those of **2**, the absorption bands of compound **1** have red-shifted significantly. This can be attributed to the decreased HOMO–LUMO energy gaps of **1** due to the remarkably extended conjugation in its molecules [39b,40].

After being fabricated into QLS films, compound **1** shows a maximal absorption band at 775 nm, which blue-shifted about 49 nm with respect to that in solution. This can be ascribed to the formation of "face-to-face" stacked "H-type" aggregates in QLS films following the exciton theory and previous results [41,42]. The orientation angle θ (Fig. S3 in Supplementary material) measured by polarized UV–vis absorption spectra is about 55.4° [43], Fig. S2a and Table S1 in Supplementary material, which is larger than 54.7°, the magic angle which is used to distinguish "H-type" aggregation from "J-type" aggregation, and suggests that the molecules of **1** in QLS films form "H-type" aggregates. The QLS film of compound **2** show also a significantly blue-shifted maximal absorption band at about 649 nm comparing with that of solution. Beside this blue-shifted absorption band, a minor band at about 734 nm, which red-shifted about 30 nm with respect to that in solution, was also found in the spectrum of compound **2** in QLS film. This absorption characteristic is caused by Davydov splitting, and implying the presence of "herringbone" structure in the QLS film of compound **2** [44–47]. The polarized UV–vis absorption spectra revealed that the orientation angle of compound **2** in QLS film is about 61.1°, which is also larger than the magic angle. Because of the special "herringbone" packing model as revealed by the absorption spectrum, this larger orientation angle is no more an indication of "H-type" aggregates, it just means that the plan of phthalocyanine rings of compound **2** are more perpendicular to the surface of the substrate than that of compound **1**. A schematic presentation for the arrangement of the molecules of **1** and **2** in QLS films are shown in Fig. S3 in Supplementary material. Obviously, the much more effective intermolecular "face-to-face" interactions in the H-aggregates of co-planar binuclear phthalocyanine **1** than that in the herringbone-arranged structure of mononuclear phthalocyanine **2** are able to provide the π electrons (as well as holes) with an extensive area for delocalization, which may benefit the charge carrier moving in the thin solid films and promote the performance of corresponding OFETs [48,49].

3.2. Electrochemical properties

The electrochemical behavior of the binuclear compound **1** was investigated by cyclic voltammetry (CV) and differential pulse voltammetry (DPV). The results are summarized in Table 1. Compound **1** presents one one-electron oxidation and two one-electron reductions in the range of −2.0 to 2.0 V. All these processes can be attributed to successive removal from, or addition of one electron to the ligand-based orbitals since the reduction of the central copper cation in this compound does not occur in this potential range [50]. The electrochemical properties of compound **2** are also investigated in the same condition. The results are the same with that reported in literature [29a]. One one-electron oxidation and two one-electron reductions within the electrochemical window of CH_2Cl_2 are observed.

As shown in Table 1, the first oxidation of **1** happens at +0.62 V, the HOMO energy level of **1** is therefore estimated to be −5.06 eV [51], which increases for about 0.52 eV with respect to that of compound **2** and matches very well with the work function of gold (−5.1 eV), and therefore, ensures the facilitation of the hole injections from Au electrodes to the phthalocyanine-based semiconductors. Nevertheless, the LUMO energy of **1** is approximately −4.24 eV deduced from the first reduction potentials, which decreases for about 0.29 eV with respect to that of **2** and just locates within the range required for air-stable n-type organic semiconductors [33,34]. This result reveals air-stable ambipolar organic semiconducting nature for compound **1** and its potential application in ambipolar OFET devices.

3.3. Film deposition and structure characterization

The information concerning the molecular ordering in the QLS films could be assessed using X-ray diffraction (XRD) technique. Out-of-plane (OOP) θ–2θ XRD scan of solution-processed films of **1** exhibits several sharp low angle diffractions with high intensities up to fifth order, revealing the long range molecular ordering across the thickness of the thin films, Fig. 2 [29d]. The *d*-spacing value estimated from the (001) diffraction peak is 3.22 nm, which can be assigned to monolayer thickness of the QLS films. Furthermore, a single family of diffraction peaks are observed without the presence of an obvious π–π stacking feature, which implies a very high crystalline order for the solution-processed films where the majority of the molecules of **1** take an edge-on orientation on the substrate with the π–π stacking direction parallel to the substrate, thereby favoring in-plane charge transport from source to drain [34]. Judging from the molecular dimensional size (the length of the octyl is not taken into account) of compound **1**, ca. 2.7 nm (length) × 1.4 nm (width) obtained from the energy-optimized structure of the molecule by using Gaussian 98 program at

Table 1
Half-wave redox potentials of **1** and **2** (V vs. SCE) in CH_2Cl_2 containing 0.1 [NBu$_4$][ClO$_4$].

Compound	Oxd$_1$	Red$_1$	Red$_2$	$\Delta E_{1/2}^0$ [a]	LUMO (eV)	HOMO (eV)
1	+0.62	−0.2	−0.87	0.82	−4.24	−5.06
2 [b]	+1.14	−0.49	−0.81	1.63	−3.95	−5.58

[a] $\Delta E_{1/2}^0$ is the potential difference between the first oxidation and first reduction processes.
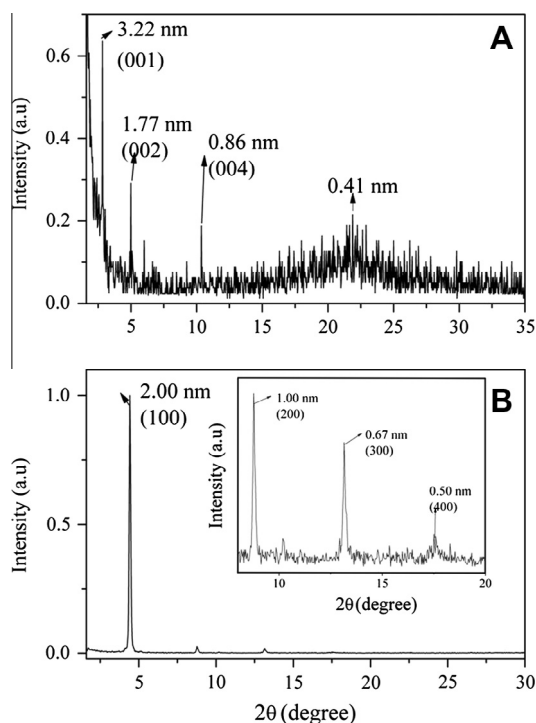[b] Cited from Ref. [29].

Fig. 2. X-ray diffraction patterns of the QLS films of **1**(A) and **2**(B) on SiO₂/Si substrate.

B3LYP/6-31G(d) level, the molecules appear to take an edge-on configuration on the substrate surface with the long axis of compound **1** perpendicular to the substrate surface. It is worth noting that the layer thickness measure by XRD experiments is larger than the length of the molecule, which can be attributed to the contribution of octyl groups to the layer thickness [52]. This result is obviously in good accordance with that deduced from UV–vis and polarized UV–vis spectroscopic measurement. Moreover, the XRD pattern displays a broad peak at the wide angle region corresponding to a d-spacing of 0.41 nm, which relates to the liquid-like order of the alkyl chains [53]. It is notable that the fact that only (00h) diffraction peaks are observed for the QLS films of compound **1**, but without giving obvious peak for the π–π stacking in the OOP XRD diagram, suggests the edge-on orientation for the molecules of **1** on the substrate with the π–π stacking direction parallel to the substrate [34]. This, in combination with the long-range ordering nature of the molecular stacking in the thin films, leads to a decrease on the energy barrier of the in plan charge transport over the QLS films.

In the low angle range of the XRD diagram of **2**, a strong diffraction peak at 2θ = 4.42° with a d spacing of 2.00 nm is found, Fig. 3B. This can be assigned to the monolayer thickness of the QLS film. Judging from the dimensional size of the molecule of compound **2**, (1.4 nm × 1.4 nm, the length of octyl group is not taken into account), the molecule of **2** seems to take edge on configuration on the surface of substrate. Due to the interdigitated octyl groups from the molecules of neighbor layer contribute also to the thickness of monolayer, the XRD measured thickness is larger than the

molecular dimensional size. In addition, the XRD pattern also displays several weaker higher order diffractions at 1.0, 0.67 and 0.5 nm, which are ascribed to diffraction from the (200), (300) and (400) planes, revealing the high molecular ordering nature of this thin film along different directions [29d].

AFM provides more information on the aspect of the QLS films and therefore allows us to correlate the morphology and electrical properties. Fig. 3 compares the morphologies of the QLS films of **1** and reference compound **2** deposited on the HMDS treated SiO₂/Si substrate. The QLS film of **1** shows uniformly distributed smooth morphology with one dimensional nanopores can be identified from the texture of the image. The QLS film of **2** presents a high uniform distributed nanosized fiber structures with distinctive boundaries between the fibers. In combination with the electronic absorption and XRD analysis results, the more uniform QLS film of **1** will significantly decrease the gaps between the grains and crack formation in the film, and thus improving the carrier mobility [54].

3.4. OFET properties

To determine the type of major carrier and the corresponding mobility of **1**, typical top-contact/bottom-gate configuration OFET devices, in which the source and drain electrodes are vacuum-deposited on the top of the QLS thin films of **1**, have been fabricated. OFET properties were evaluated under positive or negative gate bias in air to explore the majority charge carrier type, device performance, and environmental stability. Experimental data were analyzed using standard field-effect transistor equations:

$$I_{ds} = (W/2L)\mu C_0(V_G - V_T)^2 \tag{1}$$

where I_{ds} is the source–drain current, V_G the gate voltage, C_0 the capacitance per unit area of the dielectric layer, and V_T the threshold voltage [55]. The mobilities were determined in the saturation regime from the slope of plots of $(I_{ds})^{1/2}$ versus V_G. As shown in Fig. 4, the devices based on the QLS film of **1** measured in air showed ambipolar characteristics with the electron and hole mobilities of 1.7×10^{-1} cm² V⁻¹ s⁻¹ (on/off ratio: 5×10^3) and 2.3×10^{-4} cm² V⁻¹ s⁻¹ (on/off ratio: 1×10^3), respectively. In particular, the electronic or hole mobility of **1** only decreased slightly after exposure to air and remained stable for more than four weeks, which should be attributed to molecular packing effects as well as low-lying LUMO energy level (Fig. S6 in Supplementary material). As for reference **2**, only n-channel transistor behavior with a relatively lower electron mobility of 1.6×10^{-4} cm² V⁻¹ s⁻¹ and an on/off ratio of 1×10^2 [29a] was obtained in N₂ (Fig. S5 in Supplementary material). As a consequence, the changes of major charge-transport characteristics from electron to both electron and hole were successfully realized by extending π-systems of the CuPc-based molecules. The present result represents not only the first example of solution-processed, air-stable binuclear phthalocyanine-based ambipolar OFET, but more importantly provides an efficient way to enhance the performance of air-stable n-channel organic semiconductors.
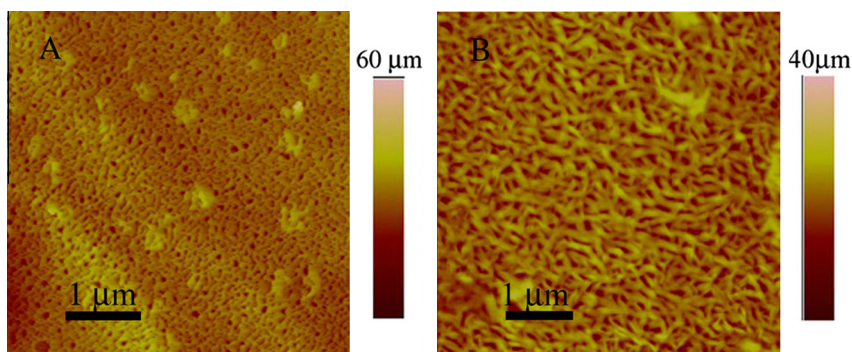
Fig. 3. AFM images of the QLS film of **1** (A) and **2** (B) on SiO$_2$/Si substrate.
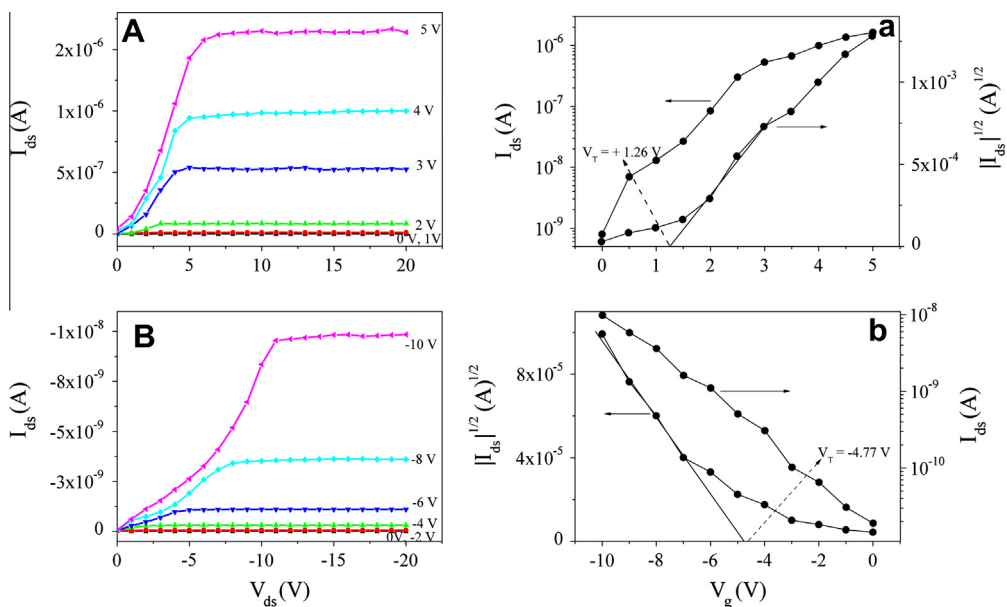

Fig. 4. Output characteristics (I_{ds} vs. V_{ds}) (A and B) and transfer characteristics ($|I_{ds}|^{1/2}$ vs. V_g) (a, V_{ds} = 10 V; b, V_{ds} = −20 V) of ambipolar OFET devices (A and a for n-channel; B and b for p-channel) based on QLS thin films of **1** deposited on HMDS-treated SiO$_2$/Si (300 nm) substrate with Au top contact model measured in air.

4. Conclusion

In summary, a soluble planar binuclear phthalocyaninato copper (II) complex, having more extended conjugation system has been designed and synthesized. The absorption spectra as well as the electrochemical data demonstrated that the HOMO/LUMO energies can be tuned successfully into the range of the requirement for an air stable ambipolar organic semiconductor. The OFET devices fabricated from the thin solid films of this binuclear phthalocyaninato copper (II) complex by solution-based QLS method performed air stable ambipolar properties with the carrier mobilities as high as 1.7×10^{-1} cm^2 V^{-1} s^{-1} for electrons and 2.3×10^{-4} cm^2 V^{-1} s^{-1} for holes, which have been significantly improved with respect to that of the OFET device based on the mononuclear phthalocyaninato copper

counterpart. This improvement can be ascribed to the extended π conjugation system and the connected electron withdrawing carboxylate groups in this binuclear phthalocyanine compound, which lower the energy of LUMO and increase the energy of HOMO efficiently. To the best of our knowledge, this represents the first example of air-stable ambipolar OFET device based on co-planar binuclear phthalocyanine derivatives fabricated by solution processing. The good OFET performance proves that co-planar binuclear phthalocyanine derivatives are very promising candidates of ambipolar semiconductors. This research not only provides a novel ambipolar organic semiconductor, but also reveals an efficient way to adjust the frontier molecular orbital energies to match the requirement of a good ambipolar organic semiconductor. Further efforts towards the design and synthesis of new co-planar

compounds and the optimization of the device fabrication are in progress in our lab.

Acknowledgements

Appendix A. Supplementary material

MALDI-TOF mass spectra of compound **1**; Polarized absorption spectra of the QLS films of **1** and **2** and the calculated orientation angles; Schematic presentation of the arrangement of the molecules of **1** and **2** in QLS film. Drain–source current (I_{ds}) versus drain–source voltage (V_{ds}) characteristic at different gate voltage for the OFET of compound **2** on the HMDS-treated SiO_2/Si substrate; The performance of the OFET of compound **1** on the HMDS-treated SiO_2/Si substrate after stored for one month at ambient temperature.

Supplementary data associated with this article can be found, in the online version, at http://dx.doi.org/10.1016/j.orgel.2013.11.017.

References

[1] C.D. Dimitrakopoulos, P.R.L. Malenfant, Adv. Mater. 14 (2002) 99.
[2] H. Sirringhaus, Adv. Mater. 17 (2005) 2411.
[3] R. Li, W. Hu, Y. Liu, D. Zhu, Acc. Chem. Res. 43 (2010) 29.
[4] H. Usta, A. Facchetti, T.J. Marks, Acc. Chem. Res. 44 (2011) 501.
[5] W. Wu, Y. Liu, D. Zhu, Chem. Soc. Rev. 39 (2010) 1489.
[6] R.P. Ortiz, A. Facchetti, T.J. Marks, Chem. Rev. 110 (2010) 205.
[7] S. Liu, W. Wang, A.L. Briseno, S.C.B. Mannsfeld, Z. Bao, Adv. Mater. 21 (2009) 1217.
[8] Y. Wang, Y. Chen, R. Li, S. Wang, X. Li, J. Jiang, Langmuir 23 (2007) 5836.
[9] C.R. Newman, C.D. Frisbie, D.A. da Silva, J.L. Bredas, P.C. Ewbank, K.R. Mann, Chem. Mater. 16 (2004) 4436.
[10] J. Zaumseil, H. Sirringhaus, Chem. Rev. 107 (2007) 1296.
[11] A. Facchetti, Mater. Today 10 (2007) 28.
[12] Z. Chen, Y. Zheng, H. Yan, A. Facchetti, J. Am. Chem. Soc. 131 (2009) 8.
[13] H. Yan, Z. Chen, Y. Zheng, C. Newman, J.R. Quinn, F. Dötz, M. Kastler, A. Facchetti, Nature 457 (2009) 67.
[14] (a) M.M. Durban, P.D. Kazarinoff, C.K. Luscombe, Macromolecules 43 (2010) 6348;
    (b) R. Madru, G. Guillaud, M. Al Saduon, M. Maitrot, C. Clarisse, C. Le Contellec, J-J. Andre, J. Simon, Chem. Phys. Lett. 142 (1987) 103.
[15] L.L. Chua, J. Zaumseil, J.F. Chang, E.C.-W. Ou, P.K.-H. Ho, H. Sirringhaus, R.H. Friend, Nature 434 (2005) 194.
[16] F.S. Kim, E. Ahmed, S. Subramaniyan, S.A. Jenekhe, ACS Appl. Mater. Interface 2 (2010) 2974.
[17] K. Walzer, B. Maennig, M. Pfeiffer, K. Leo, Chem. Rev. 107 (2007) 1233.
[18] (a) M.A. Baldo, M.E. Thompson, S.R. Forrest, Nature 403 (2000) 750;
    (b) M.A. Baldo, D.F. O'Brien, Y. You, A. Shoustikov, S. Sibley, M.E. Thompson, S.R. Forrest, Nature 395 (1998) 151.
[19] (a) Y. Zhang, X. Cai, Y. Bian, J. Jiang, Struct. Bond. 135 (2010) 275;
    (b) Y. Sun, Y. Liu, D. Zhu, J. Mater. Chem. 15 (2005) 53.
[20] (a) Z. Bao, A.J. Lovinger, A. Dodabalapur, Appl. Phys. Lett. 69 (1996) 3066;
    (b) K. Xiao, Y. Liu, G. Yu, D. Zhu, Appl. Phys. A 77 (2003) 367;
    (c) K. Xiao, Y. Liu, G. Yu, D. Zhu, Synth. Met. 137 (2003) 991;
    (d) J. Yuan, J. Zhang, J. Wang, X. Yan, D. Yan, W. Xu, Appl. Phys. Lett. 82 (2003) 3967;
    (e) J. Wang, X. Yan, Y. Xu, J. Zhang, D. Yan, Appl. Phys. Lett. 85 (2004) 5424;
    (f) K. Xiao, Y. Liu, Y. Guo, G. Yu, L. Wan, D. Zhu, Appl. Phys. A 80 (2005) 1541;
    (g) X. Yan, H. Wang, D. Yan, Thin Solid Films 515 (2006) 2655;
    (h) Z. Bao, A.J. Lovinger, A. Dodabalapur, Adv. Mater. 9 (1997) 42;
    (i) R. Zeis, T. Siegrist, C. Kloc, Appl. Phys. Lett. 86 (2005) 22103;
    (j) Q. Tang, H. Li, M. He, W. Hu, C. Liu, K. Chen, C. Wang, Y. Liu, D. Zhu, Adv. Mater. 18 (2006) 65.
[21] W. Hu, Y. Liu, Y. Xu, S. Liu, S. Zhou, D. Zhu, Synth. Met. 104 (1999) 19.
[22] K. Xiao, Y. Liu, X. Huang, Y. Xu, G. Yu, D. Zhu, J. Phys. Chem. B 107 (2003) 9226.
[23] (a) Y. Chen, W. Su, M. Bai, J. Jiang, X. Li, Y. Liu, L. Wang, S. Wang, J. Am. Chem. Soc. 127 (2005) 15700;
    (b) W. Su, J. Jiang, K. Xiao, Y. Chen, Q. Zhao, G. Yu, Y. Liu, Langmuir 21 (2005) 6527;
    (c) R. Li, P. Ma, S. Dong, X. Zhang, Y. Chen, X. Li, J. Jiang, Inorg. Chem. 46 (2007) 11397;
    (d) Y. Chen, R. Li, R. Wang, P. Ma, S. Dong, Y. Gao, X. Li, J. Jiang, Langmuir 23 (2007) 12549;
    (e) Y. Gao, P. Ma, Y. Chen, Y. Zhang, Y. Bian, X. Li, J. Jiang, C. Ma, Inorg. Chem. 48 (2009) 45.
[24] (a) C.R. Newman, C.D. Frisbie, D.A. da Silva Filho, J.-L. Brédas, P.C. Ewbank, K.R. Mann, Chem. Mater. 16 (2004) 4436;
    (b) G. Guillaud, M. Al Saduon, M. Maitrot, J. Simon, M. Bouvet, Chem. Phys. Lett. 167 (1990) 503.
[25] Z. Bao, A.J. Lovinger, J. Brown, J. Am. Chem. Soc. 120 (1998) 207.
[26] D.G. de Oteyza, E. Barrena, J.O. Ossó, H. Dosch, S. Meyer, J. Pflaum, Appl. Phys. Lett. 87 (2005) 183504.
[27] Y. Sakamoto, T. Suzuki, M. Kobayashi, Y. Gao, Y. Fukai, Y. Inoue, F. Sato, S. Tokito, J. Am. Chem. Soc. 126 (2004) 8138.
[28] Q. Tang, H. Li, Y. Liu, W. Hu, J. Am. Chem. Soc. 128 (2006) 14634.
[29] (a) P. Ma, J. Kan, Y. Zhang, C. Hang, Y. Bian, Y. Chen, N. Kobayshi, J. Jiang, J. Mater. Chem. 21 (2011) 18552;
    (b) J. Kan, Y. Chen, D. Qi, Y. Liu, J. Jiang, Adv. Mater. 24 (2012) 1755;
    (c) J. Kan, Y. Chen, J. Gao, L. Wan, T. Lei, P. Ma, J. Jiang, J. Mater. Chem. 22 (2012) 15695;
    (d) D. Li, H. Wang, J. Kan, W. Lu, Y. Chen, J. Jiang, Org. Electron. 14 (2013) 2582.
[30] H. Usta, C. Risko, Z. Wang, H. Huang, M.K. Deliomeroglu, A. Zhukhovitskiy, A. Facchetti, T.J. Marks, J. Am. Chem. Soc. 131 (2009) 5586.
[31] (a) Y. Guo, G. Yu, Y. Liu, Adv. Mater. 22 (2010) 4427;
    (b) P. Sonar, S.P. Singh, Y. Li, M.S. Soh, A. Dodabalapur, Adv. Mater. 22 (2010) 5409.
[32] B.A. Jones, A. Facchetti, M.R. Wasielewski, T.J. Marks, J. Am. Chem. Soc. 129 (2007) 15259.
[33] M.L. Tang, J.H. Oh, A.D. Reichardt, Z. Bao, J. Am. Chem. Soc. 131 (2009) 3733.
[34] X. Guo, R.P. Ortiz, Y. Zheng, Y. Hu, Y.-Y. Noh, K.-J. Baeg, A. Facchetti, T.J. Marks, J. Am. Chem. Soc. 133 (2011) 1405.
[35] A. Facchetti, M. Mushrush, H.E. Katz, T.J. Marks, Angew Chem. Int. Ed. 15 (2003) 33.
[36] Y. Chen, M. Bouvet, T. Sizun, Y. Gao, C. Plassard, E. Lesniewska, J. Jiang, Phys. Chem. Chem. Phys. 12 (2010) 12851.
[37] S.E. Maree, T. Nyokong, J. Porphyrins Phthalocyanines 5 (2001) 782.
[38] B.N. Achar, G.G. Fohlen, J.A. Parker, J. Polym. Sci. Polym. Chem. 20 (1982) 1785.
[39] (a) N. Kobayashi, F. Takamitsu, D. Lelièvre, Inorg. Chem. 39 (2000) 3632;
    (b) S.G. Makarov, O.N. Suvorovaa, D. Wöhrle, J. Porphyrins Phthalocyanines 15 (2011) 791.
[40] M. Yoon, S.A. DiBenedetto, M.T. Russell, A. Facchetti, T.J. Marks, Chem. Mater. 19 (2007) 4864.
[41] M. Kasha, H.R. Rawls, M.A. El-Bayoumi, Pure Appl. Chem. 11 (1965) 371.
[42] N. An, Y. Shi, J. Feng, D. Li, J. Gao, Y. Chen, X. Li, Org. Electron. 14 (2013) 1197.
[43] Y. Qiao, Y. Guo, C. Yu, F. Zhang, W. Xu, Y. Liu, D. Zhu, J. Am. Chem. Soc. 134 (2012) 4084.
[44] W. Chen, W. Ko, Y. Chen, C. Cheng, C. Chan, K. Lin, Langmuir 26 (2010) 2191.
[45] M. Wojdyla, B. Derkowska, M. Rebarz, A. Bratkowski, W. Bala, J. Opt. A: Pure Appl. Opt. 7 (2005) 463.
[46] B.M. Hassan, H. Li, N.B. McKeown, J. Mater. Chem. 10 (2000) 39.
[47] (a) Y. Chen, S. Zhao, X. Li, J. Jiang, J. Colloid Interface Sci. 289 (2005) 200;
    (b) Y. Chen, M. Bouvet, T. Sizun, G. Barochi, J. Rossignol, E. Lesniewska, Sensor Actuat. B-Chem. 155 (2011) 165.
[48] J.E. Anthony, J.S. Brooks, D.L. Eaton, S.R. Parkin, J. Am. Chem. Soc. 123 (2001) 9482.
[49] J. Locklin, K. Shinbo, K. Onishi, F. Kaneko, Z. Bao, R.C. Advincula, Chem. Mater. 15 (2003) 1404.

[50] A.J. Bard, R. Parsons, J. Jordan, Standard Potentials in Aqueous Solution, (eds.), Marcel Dekker, New York, 38 (1985) 127.

[51] SCE energy level is −4.44 eV below the vacuum level. A.J. Bard, L.R. Faulkner, in: Electrochemical methods-fundamentals and applications, Wiley, New York, 1984.

[52] K. Balakrishnan, A. Datar, T. Naddo, J. Huang, R. Oitker, M. Yen, J. Zhao, L. Zang, J. Am. Chem. Soc. 128 (2006) 7390.

[53] (a) F. Würthner, C. Thalacker, S. Diele, C. Tschierske, Chem. Eur. J. 7 (2001) 2245;
(b) H. Wu, L. Xue, Y. Shi, Y. Chen, X. Li, Langmuir 27 (2011) 3074.

[54] J.H. Oh, S. Liu, Z. Bao, R. Schmidt, F. Würthner, Appl. Phys. Lett. 91 (2007) 212107.

[55] S.M. Sze, Physics of Semiconductor Devices, second ed., John Wiley & Sons, New York, 1981.